Brain Struct Funct (2010) 214:339–353
DOI 10.1007/s00429-010-0247-z

ORIGINAL ARTICLE

Cytoarchitectonic and chemoarchitectonic characterization of the prefrontal cortical areas in the mouse

H. J. J. M. Van De Werd · G. Rajkowska · P. Evers · Harry B. M. Uylings

Received: 4 August 2009 / Accepted: 18 February 2010 / Published online: 12 March 2010

Abstract This study describes cytoarchitectonic criteria to define the prefrontal cortical areas in the mouse brain (C57BL/6 strain). Currently, well-illustrated mouse brain stereotaxic atlases are available, which, however, do not provide a description of the distinctive cytoarchitectonic characteristics of individual prefrontal areas. Such a description is of importance for stereological, neuronal tracing, and physiological, molecular and neuroimaging studies in which a precise parcellation of the prefrontal cortex (PFC) is required. The present study describes and illustrates: the medial prefrontal areas, i.e., the infralimbic, prelimbic, dorsal and ventral anterior cingulate and Fr2 area; areas of the lateral PFC, i.e., the dorsal agranular insular cortical areas and areas of the ventral PFC, i.e., the lateral, ventrolateral, ventral and medial orbital areas. Each cytoarchitectonically defined boundary is corroborated by one or more chemoarchitectonic stainings, i.e., acetylcholine esterase, SMI32, SMI311, dopamine, parvalbumin, calbindin and myelin staining.

Keywords Cortical parcellation · Infralimbic, prelimbic, anterior cingulate, Fr2, agranular insular and orbital cortical areas · Nissl · Myelin · Acetylcholinesterase · Dopamine · Calcium binding proteins · SMI-32 · SMI-311

Abbreviations

ACd	Dorsal agranular cingulate area
ACv	Ventral agranular cingulate area, dorsal and ventral part
AId_1	Dorsal agranular insular area, dorsal part
AId_2	Dorsal agranular insular area, ventral part
AIv	Ventral agranular insular area
AIp	Posterior agranular insular area
CB	Calbindin
CL	Claustrum
cc	Corpus callosum
DA	Dopamine
DI	Dysgranular insular area
DLO	Dorsolateral orbital area
FPl	Lateral frontal polar area
FPm	Medial frontal polar area
Fr1	Frontal area 1
Fr2	Frontal area 2
GI	Granular insular area
IG	Indusium griseum
IL	Infralimbic area
LO	Lateral orbital area
MO	Medial orbital area
OB	Olfactory bulb

H. J. J. M. Van De Werd · H. B. M. Uylings (✉)
Department of Anatomy and Neuroscience,
VU University Medical Center, P.O. Box 7057,
1007 MB Amsterdam, The Netherlands
e-mail: hbm.uylings@vumc.nl

H. J. J. M. Van De Werd · H. B. M. Uylings
Graduate School Neuroscience Amsterdam,
Amsterdam, The Netherlands

G. Rajkowska
Department of Psychiatry and Human Behavior, University of Mississippi Medical Center, Jackson, MS, USA

P. Evers
Netherlands Brain Bank, KNAW, Amsterdam, The Netherlands

H. B. M. Uylings
Department of Psychiatry and Neuropsychology,
School for Mental Health and Neuroscience,
Maastricht University, Maastricht, The Netherlands

PFC	Prefrontal cortex
PL	Prelimbic area
PV	Parvalbumin
RSA	Agranular retrosplenial cortex
RSG	Granular retrosplenial cortex
VLO	Ventrolateral orbital area
VLO_p	Posterior ventrolateral orbital area
VO	Ventral orbital area

Introduction

Only a few publications, describing cytoarchitectonic features of the mouse cerebral cortex, have been found in literature (Rose 1929; Caviness 1975; Wree et al. 1983). None of these studies has focused on the prefrontal cortex (PFC), in contrast to studies of the rat PFC (Krettek and Price 1977; Van Eden and Uylings 1985; Uylings and Van Eden 1990; Ray and Price 1992; Reep et al. 1996; Van De Werd and Uylings 2008). The available mouse cytoarchitectonic/stereotaxic atlases (Franklin and Paxinos 2008; Hof et al. 2000; Slotnick and Leonard 1975) provide fine architectonic figures, but given their scope do not describe the cytoarchitectonic criteria for the parcellation of the PFC.

The cytoarchitectonic definition of mouse prefrontal areas is essential for stereological studies on the total number of neurons and/or glia cells in the distinct cortical areas using Nissl stainings (e.g., Rajkowska et al. 2004). In addition, this is necessary in studies examining the question whether a differential pattern of connectivity with cortical, striatal and thalamic regions corresponds to different cytoarchitectonically defined cortical areas (Uylings et al. 2003; Groenewegen and Witter 2004). In these and also in physiological studies, different cytoarchitectonic prefrontal areas need to be defined applying consistent and reproducible criteria. Finally, such a cytoarchitectonic study is needed due to the present intensive use of mice as animal models for human brain disorders.

This study aims to provide cytoarchitectonic criteria to characterize the boundaries between different cortical areas in the medial, lateral and ventral/orbital regions of the mouse PFC. As in other studies (e.g., Van de Werd and Uylings 2008), the cytoarchitectonic boundaries are compared with boundaries visible in chemoarchitectonic stainings for myelin, acetylcholinesterase (AChE), dopaminergic fibers, SMI-32, SMI-311 and parvalbumin (PV) and calbindin (CB)-positive neurons.

Materials and methods

The cytoarchitecture of the PFC was studied in ten adult, male mice (strain C57BL/6) of similar weight (approximately 20 g). These control mouse brains were kindly donated and immersion fixed by Dr. H. Manji, NIMH, USA. All animal procedures were in strict accordance with the NIH animal care guidelines. The histological processing of these brains was performed at the laboratory of Dr. Rajkowska. The brains were embedded in 12% celloidin, cut into 40-μm serial sections using a sliding microtome and Nissl (1% cresyl violet) stained. Celloidin was chosen as an embedding medium to allow for the preparation of 'thick' sections with clear morphology and high contrast of Nissl-stained neurons and glial cells. In these immersion-fixed brains, any spots showing pycnotic reaction were not incorporated in this study.

In addition to these ten mice, four adult male mice (C57BL/6 strain) were stained for dopamine and four adult male mice for AChE, myelin, and immunohistochemically for SMI, PV and CB. For each staining, a different set of sections with several consecutive sections stained with Nissl at HBMU's laboratory was used. The antibodies applied were the dopamine (DA) antibody (Geffard et al. 1984), SMI-32 antibody (Sternberger Monoclonals Inc., Baltimore, MD, USA: monoclonal antibody to one epitope of non-phosphorylated tau neurofilaments, lot number 11), SMI-311antibody (pan-neuronal neurofilament marker cocktail of several monoclonal antibodies for several epitopes of non-phosphorylated tau protein, Sternberger Monoclonals Inc., Baltimore, MD, USA: lot number 9) (SMI antibodies are presently distributed through Covance Research Products, USA), monoclonal anti-CB D-28K antibody (Sigma, St. Louis, MO, USA: product number C-9848, clone number CB-955, lot number 015K4826), and monoclonal anti-PV antibody (Sigma, St. Louis, MO, USA: product number P-3171, clone number PA-235, lot number 026H4824). Mice to be stained for DA were intracardially perfused under deep pentobarbital anesthesia (1 ml/kg body weight, i.p.), with saline followed by fixative. For DA staining, the fixative was 5% glutaraldehyde in 0.05 M acetate buffer at pH 4.0. After perfusion, the brains were immersed in 0.05 Tris containing 1% sodium disulfite ($Na_2S_2O_5$) at pH 7.2 (De Brabander et al. 1992). Mouse PFC was sectioned at 40 μm by a vibratome. These sections were stained overnight in a cold room at 4°C using the polyclonal primary antibody sensitive to DA that was raised in the Netherlands Institute for Brain Research (NIBR) (Geffard et al. 1984), the specificity of which had been demonstrated previously (Kalsbeek et al. 1990). DA antiserum was diluted 1:2,000 in 0.05 M Tris containing 1% $Na_2S_2O_5$ and 0.5% Triton X-100, pH 7.2. After overnight incubation, the sections were washed three times with Tris-buffered saline (TBS) and subsequently incubated in the secondary antibody goat–antirabbit, also raised in NIBR at 1:100 for 1 h. After having been rinsed 3× in TBS, it was incubated in the tertiary antibody, peroxidase–

antiperoxidase, at 1:1,000 for 60 min. Both the secondary and the tertiary antibodies were diluted in TBS with 0.5% gelatine and 0.5% Triton X-100. For visualization, the sections were transferred into 0.05% diaminobenzidine (DAB; Sigma) with 0.5% nickel ammonium sulfate. The reaction was stopped after a few minutes by transferring the sections to TBS (3 × 10 min), then the sections were mounted on slides, air dried, washed, dehydrated and coverslipped.

Mice to be stained with anti-PV, anti-CB and SMI-32 and SMI-311 were fixed with 4% formaldehyde solution in 0.1 M phosphate buffer at pH 7.6. Mouse PFC was sectioned at 40 μm by a vibratome. To prevent endogenous peroxidase activity, free-floating sections were pretreated for 30 min in a Tris-buffered saline (TBS) solution containing 3% hydrogen peroxide and 0.2% Triton X-100. To prevent non-specific antibody staining, these sections were placed in a milk solution (TBS containing 5% nonfat dry milk and 0.2% Triton X-100) for 1 h. Incubation of the primary antibody, directly after the milk step was carried out overnight in a cold room at 4°C. The primary antibodies were diluted in the above-mentioned milk solution: SMI-32 and SMI-311 at 1:1,000, PV antibody at 1:1,000, and CB antibody at 1:250. For the monoclonal SMI-32, SMI-311, PV and CB antibodies, raised in mice, we used peroxidase-conjugated rabbit–antimouse (1:100 in 5% milk solution with 0.2% Triton X-100) as a secondary antibody. Visualization took place in 0.05% diaminobenzidine enhanced with 0.2% nickel ammonium sulfate. The reaction was stopped after a few minutes by transferring these sections to TBS (3 × 10 min), after which the sections were rinsed in distilled water, mounted on slides, air dried, washed, dehydrated and coverslipped. Control sections that were incubated according to the same procedure as described above, omitting the primary antibody, were all negative. All sections were cut coronally, because the coronal plane offers in general the best view to differentiate between the subareas of the rodent PFC (Uylings et al. 2003; Van de Werd and Uylings 2008).

Sections were processed for AChE staining according to the protocol described by Cavada et al. (1995). The sections were incubated overnight in a solution of cupric sulfate and acetate buffer at pH 5 to which acetylthiocholine iodide and ethopropazine were added just before the start of incubation. After rinsing, the sections were developed in a sodium sulfide solution until a light brown color appeared and subsequently intensified to a dark brown color in a silver nitrate solution. Finally, the sections were differentiated after rinsing in a thiosulfate solution, dehydrated and mounted. In all steps, the solutions and sections were shaken constantly. The myelin was stained with silver by physical development according to Gallyas (1979). The sections were first placed in 100% ethanol and then immersed in a 2:1 solution of pyridine and acetic acid for 30 min. After rinsing, they were placed in an ammonium silver nitrate solution and after rinsing with 0.5% acetic acid, the sections were immersed in the optimal physical developer solution at room temperature (Gallyas 1979) until they showed good stain intensity under the microscope. Then the development of the staining was stopped in 0.5% acetic acid and the sections were dehydrated and mounted with Histomount. The sections were studied at intervals of 80–160 μm, and examined under a light microscope at a 63× magnification.

Nomenclature

Our PFC nomenclature is mainly based on the one used for the rat PFC by Krettek and Price (1977), Uylings and Van Eden (1990), Ray and Price (1992), Reep et al. (1996), Uylings et al. (2003) and Van De Werd and Uylings (2008). Some names used for areas of the rat PFC have been left out by us because they could not be distinguished from other areas having different names (see below).

Results

In mice, as in rats, the PFC is defined as the agranular part of the frontal lobe. On the lateral side of the frontal lobe, the dorsal part of the dorsal agranular insular area (AId1), borders on the (dys)granular insular cortex (DI/GI), while on the mediodorsal side, the second frontal area, Fr2, borders on the (dys)granular cortex (Fr1). The position of the subareas of the PFC are shown in Fig. 1, while in Fig. 2 in the rostrocaudal coronal sections, the PFC subareas are shown.

Medial areas

Border between the prefrontal area Fr2 and the (dys)granular area Fr1

In the medial part of Fr1, layer V moves to a more superficial position due to the gradual disappearance of layer IV. We take the medial end of this shift as the location where the granular layer IV has disappeared completely, thus more medially than the visual appearance of layer IV. At the border on Fr2, layer V has reached its most superficial position. This is the main characteristic of the Fr1–Fr2 boundary. In Fr2, the cells of layer II are, as a layer, more clearly separated from layer I, while in Fr1 layer II shows clefts (Figs. 3, 4). In Fr2, the columns of the layers V and VI are clearly situated closer to each other than in Fr1 (e.g., Fig. 4a). In Fr2, the cells of the layer VI

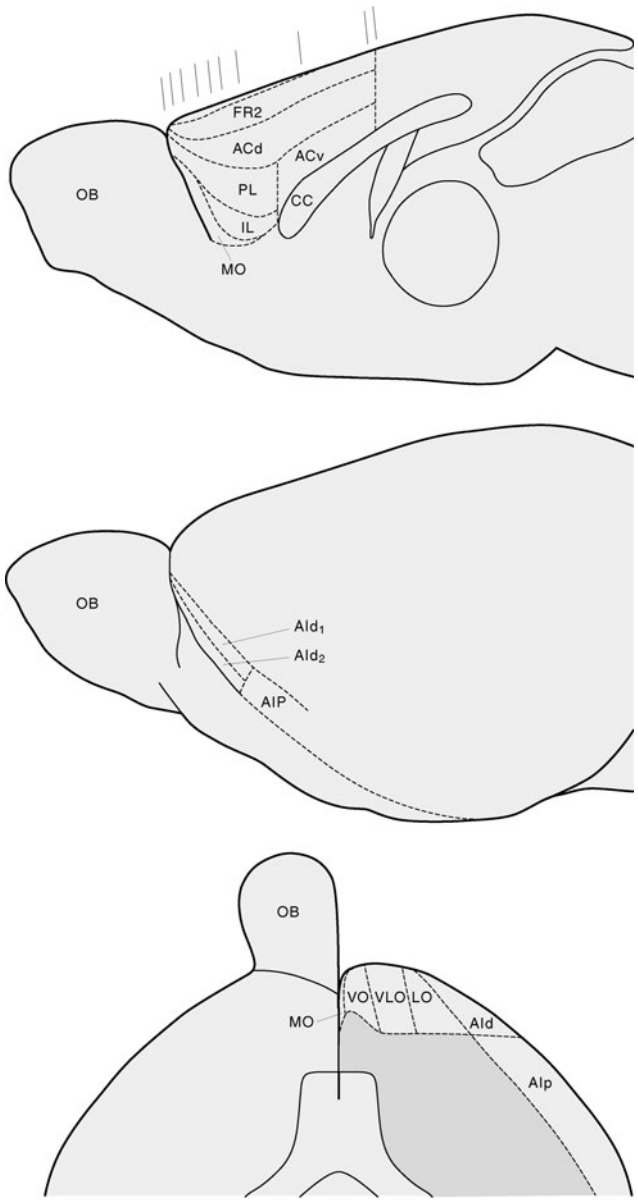

Fig. 1 Schematic view of PFC areas. *Top panel* medial view; *middle panel* lateral view; and *lower panel* orbital view. The *lines* above the medial view mark the positions of the ten sections shown in Fig. 2. For abbreviations, see "Abbreviations"

are always in columns, while in Fr1, instead of columns a horizontal arrangement of cells might be present. The cells of the layer V of Fr2 are smaller than those of Fr1 (Figs. 3, 4, 5a).

Border between Fr2 and dorsal anterior cingulate areas

In Fr2, the outer surface of layer II is generally smooth, but in dorsal agranular cingulate area (ACd) it is irregular and has a darker, denser appearance (Figs. 3, 4, 5a). The columns that can readily be seen in the layers V and VI of both Fr2 and ACd are more densely packed in ACd than in Fr2 (Figs. 3, 4, 5a). In Fr2, layer III tends to be broader and lighter in appearance than in ACd (e.g., Fig. 4b).

Border between dorsal anterior cingulate and prelimbic areas

The main characteristic of the border between ACd and prelimbic (PL) is the columnar arrangement of layer V cells in ACd, while in PL the cells of the layer V appear in disorderly arrangement (Figs. 3, 4a, b, 6a). Layer VI in ACd shows columns, while in PL the cells of the layer VI are mainly arranged in horizontal rows (Figs. 3, 4a, b, 6a). In ACd, layer II is narrow with its cells mostly concentrated at the boundary with layer I, while in PL, layer II is a little broader with its cells more equally spread over the layer. Layer III of ACd is lighter in appearance than layer III of PL, due to the number of cells in ACd being less dense than in PL (e.g., Fig. 4b).

Distinction in prelimbic between PLd and PLv

In PL, we discern a dorsal and a ventral part based on a different aspect of layer II, which is narrow and compact in the dorsal part of PL, but broad and less compact in the ventral part. Layers III and V are more compact in the ventral part of PL. The transition is rather sharp and marked in our pictures by a small arrow (Figs. 3, 4, 6, 7).

Border between prelimbic and infralimbic areas

In PL, the layers II, III and V are clearly distinguishable, i.e., the dark layer II is separated from layer V by the lighter layer III, whereas in IL these layers are more or less homogeneous. In IL, the size and distribution of the cells of layers II, III and V are about the same. A typical feature of IL is that cells of layer II in IL spread far into layer I, while in PL only few cells of layer II are seen in layer I (Figs. 4 a, b, 6). Therefore, layer II appears wider in IL than in PL. In addition, the size of the somata in layer II in IL appears smaller than in PL (e.g., Fig. 6).

Border between prelimbic and medial orbital areas

PL borders ventrally on medial orbital (MO) area only in the anterior part of the frontal lobe (i.e., level a, b and c in Figs. 1, 2). In MO, the cells are more homogeneously distributed in layer II, while in PL they are unevenly spread over layer II with the cells more densely packed on the boundary with layer I (Fig. 3). In addition, the border between layer II and III is less difficult visible in MO than in ventral PL (Fig. 3).

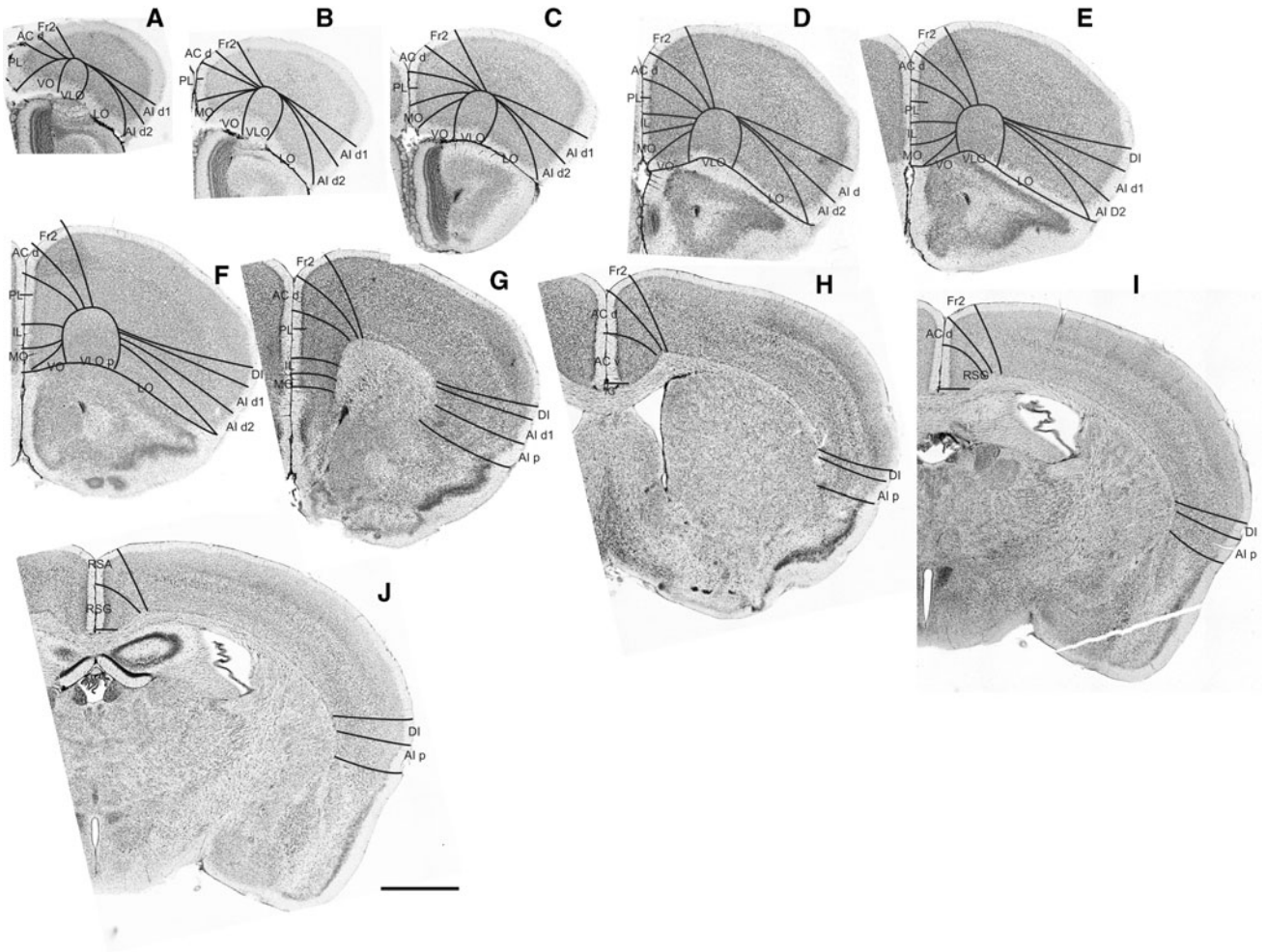

Fig. 2 Overview of PFC subareas in Nissl-stained sections at ten different levels indicated in Fig. 1. For abbreviations, see "Abbreviations". *Scale bar* 1 mm

Border between infralimbic and medial orbital areas

Caudal to panel c in Fig. 2, IL borders on MO. In IL the layers II, III and V are homogeneous, while in MO those layers can be distinguished from each other (e.g., Figs. 4b, 6b). This difference between IL and MO is most evident in the transition of layer II into layer III (Figs. 4 a, b, 6).

Border between dorsal and ventral anterior cingulate areas

At the level of genu (Figs. 1, 2), MO and IL have disappeared and PL changes into ventral agranular cingulate area, dorsal and ventral part (ACv). Thus, caudal to genu, ACd borders on ACv. In ACd, cells are arranged in columns, while in ACv they are not. This is especially clear in layer VI, which is columnar in ACd, while in ACv the cells are mainly arranged in horizontal rows (Figs. 4c, 5a). Layers II and III in areas ACd and ACv differ less from each other than they do between ACd and PL. The somata in layers III and V in ACd are generally larger than those in ACv (Figs. 4c, 5a).

The difference between prelimbic and ventral anterior cingulate areas

Generally, PL is more densely packed than ACv (Figs. 3, 4a, b, 6 for PL and Figs. 4c, 5a for ACv). In PL, the layers are less distinguishable than in ACv. In ACv, the horizontal laminar arrangement of cells in layer VI is well distinguishable from the cells of layer V that are larger and less densely packed than in PL (Fig. 4). Layer III in ACv has a lighter appearance than layer III in PL, due to the less dense packing of cells in ACv. As a consequence, ACv and ACd differ less than ACd and PL. The transition of PL into ACv, however, is a gradual

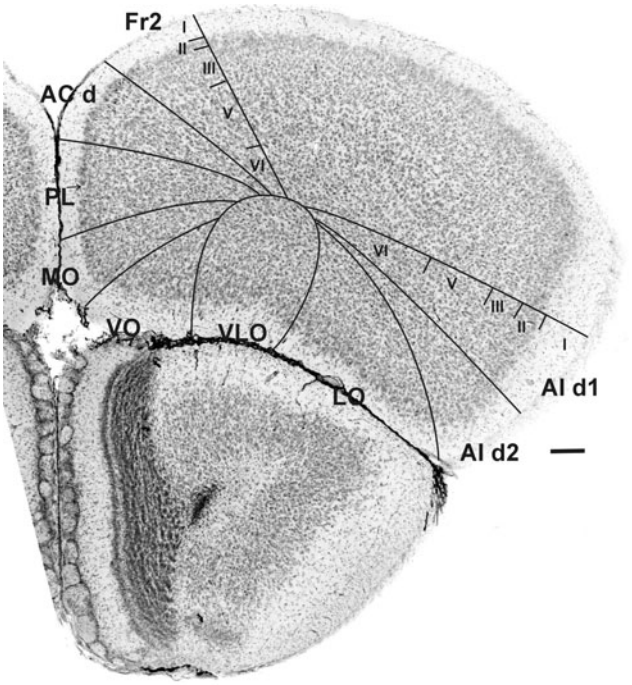

Fig. 3 Section through the frontal pole. In the medial part of granular Fr1, layer V moves to a more superficial position due to the diminishing layer IV. In Fr2, the cells of layer II are more homogeneously separated from layer I than in Fr1. In ACd and in dorsal PL, the cells of layer II are densely packed on the border with layer I, but the cells of layer III are more densely packed in PL than in ACd. *Arrow* indicates the border between dorsal PL and ventral PL. In ventral PL, layer II is wider and less densely packed. In VLO, the columns in layers II and III distinguish this area from VO and LO. See also the clustering of layer II cells in LO, the wide loosely packed cells of layer II in AId 2 and the densely packed layer II of AId1. *Scale bar* 150 μm

process. Usually, PL changes into ACv at the genu of the corpus callosum.

Distinction between the dorsal and ventral part in ACv

As in PL, we can discern a difference between the dorsal and ventral part in ACv. In the dorsal part, layer II is narrower with some clustering and with the layers III, V and VI less compact than in the ventral part (Figs. 4c, 5a). Layer II in the ventral part is broader with sometimes an aspect of a spindle (e.g., Fig. 4c). Layer VI in the ventral part of ACv is often darker than in the dorsal part of ACv. In Figs. 4c and 5a, the border between the dorsal and ventral part of ACv is marked by a small arrow.

Caudal border of the medial prefrontal areas and the retrosplenial cortex

The first appearance of the fine, darkly stained granules in layers II–III marks the transition of ACv into the granular retrosplenial region (RSG). The agranular area dorsally to RSG is the agranular retrosplenial area (RSA). For comparison of the cortex of the PFC with the retrosplenial cortex see Fig. 5a, b.

Lateral areas

Border between the dysgranular insular cortex or granular insular cortex and the dorsal agranular insular areas

In DI, layer IV is homogeneous with layers II and III, and in the GI, layer IV is well distinguished from the layers III and V by its small, densely and equally dispersed cells. In AId_1, layer IV is absent and the layers II, III, and V are well distinguished from each other. Layer II is broad, dark and compact in AId_1, while homogeneous with layers III and IV in DI and less compact in GI. In AId_1, the cells of the layersV and VI have been arranged in columns, but not in DI or GI. In AId_1, layer V lies more closely to the surface than in DI or GI due to lack of layer IV (Figs. 3, 8, 9a).

Two subareas in the AId: dorsal AId_1 and ventral AId_2

The layer II of AId_1 has a dark and compact appearance, while in dorsal agranular insular area, ventral part (AId_2) layer II is less compact and some of its cells spread into layer I. In AId_2, the columns of the layers V and VI are more densely packed than in AId_1 (Figs. 3, 8).

Border between the dorsal part of the AId_1 and the posterior agranular insular areas

In AId_1, the transition from one layer of the cortex to another is gradual, while in posterior agranular insular area (AIp) the layers appear to be clearly separated from each other and are more compact than in AId_1. This gives the impression of eight or more layers, including the claustrum. In AId_1, the cells are arranged in columns but not in AIp (Fig. 9a).

More caudally, when AId becomes progressively smaller and ultimately disappears, AIp borders directly on DI (Fig. 9b).

Ventral or orbital areas

Border between the ventral part of the dorsal agranular insular and the lateral orbital areas

In AId_2, layer II is broad, the cells are not densely packed and some cells extend into layer I; in LO, layer II is narrow and its cells form clusters (Figs. 3, 8). These are the main characteristics that distinguish AId_2 from LO. In AId_2 the

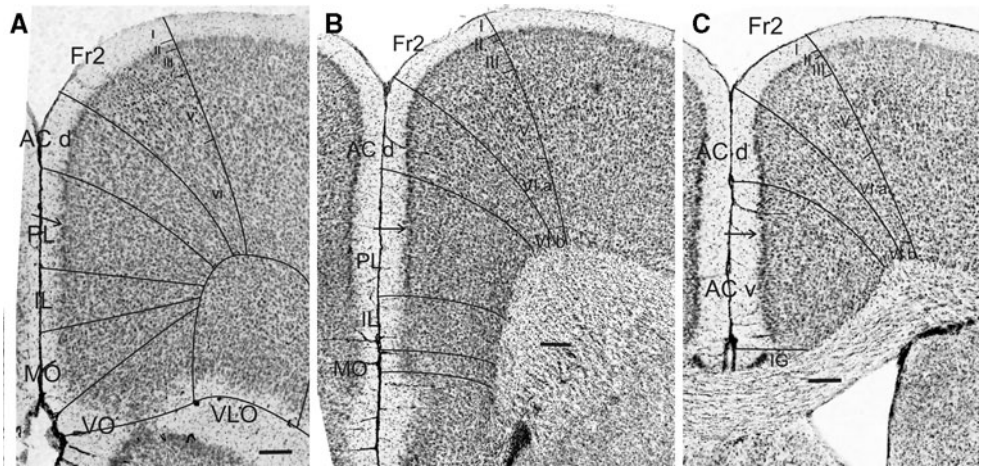

Fig. 4 **a** Medial PFC at the fusion of the frontal lobe with the retrobulbar region. Layer III cells in ACd are less densely packed than in PL. *Arrow* indicates the border between dorsal and ventral PL. Layer II in the ventral PL is wider than in the dorsal PL. The cells of layer II are evenly dispersed in MO, but its boundary on layer I and III is less sharp than in Fig. 3. Layer II of area IL extends into layer I. The *columns* in layers II and III of VLO are typical. **b** Medial PFC at the level of the forceps minor of corpus callosum. In Fr2 and ACd, the layer VI shows columns, while a horizontal arrangement is visible in PL, IL and MO parallel to pia. *Arrow* indicates the border between the dorsal and ventral PL C Medial PFC at the supragenual level. In ACd note that layers II and III are denser than in Fr2 and ACv. The *columns* in ACd are denser in VI and V than in Fr2. *Arrow* indicates the border between the dorsal ACv and ventral ACv. Layer II is wider in the ventral ACv and layer VI cells are not in columns, but rather in a horizontal arrangement. *Scale bars* 150 μm

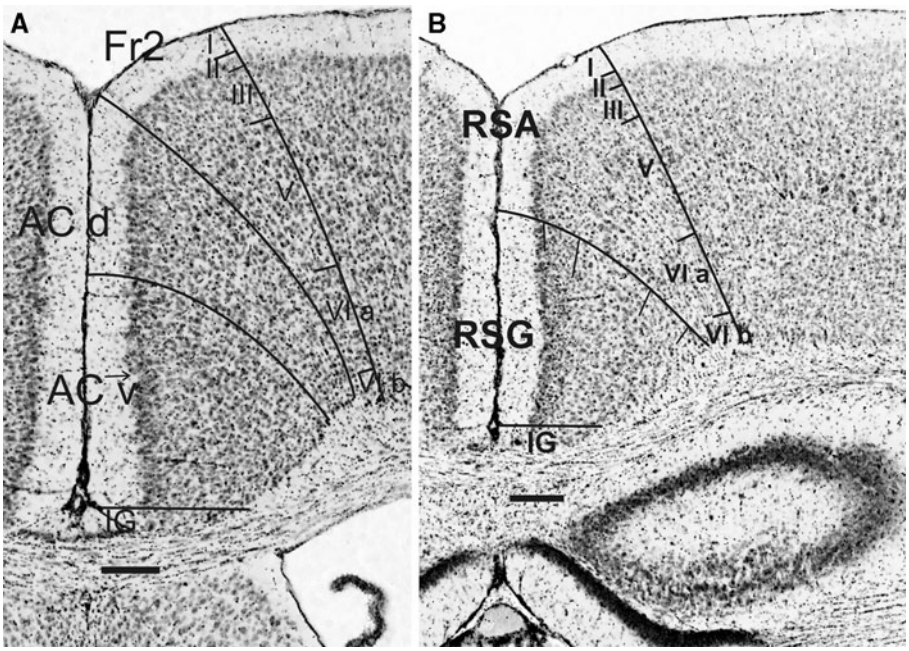

Fig. 5 **a** Medial PFC just anterior to **i** in Fig. 2. The highest point of layer V and a change in layer II are the indications for the boundary between Fr2 and Fr1. The columns in layer VI and the densely packed cells in layer II in ACd differ from the horizontal arrangement of layer VI cells and the wide layer II in ACv. *Arrow* indicates the border between dorsal ACv and ventral ACv. **b** Section through the retrosplenial region at the level of **j** in Fig. 2. *Scale bars* 150 μm

cells of the layers III and V are arranged in columns, but not in LO (Figs. 3, 8a). Layer I of LO is narrower than layer I of AId $_2$ (Figs. 3, 8a).

Border between lateral orbital and ventrolateral areas

In LO, layer II shows clustering of cells and a sharp boundary with layer III, while in VLO the cells of the layers II and III show columns and the layers II and III are homogeneous. In VLO, columns are sometimes seen in layer V, but not in layer V in LO. On the whole, VLO is more homogeneous than LO, so its layers are less distinguishable than in LO (Figs. 3, 8).

The homogeneity of the layers in VLO is nearly total in the most posterior part of VLO, justifying the description VLOp for this part of VLO (Fig. 8b).

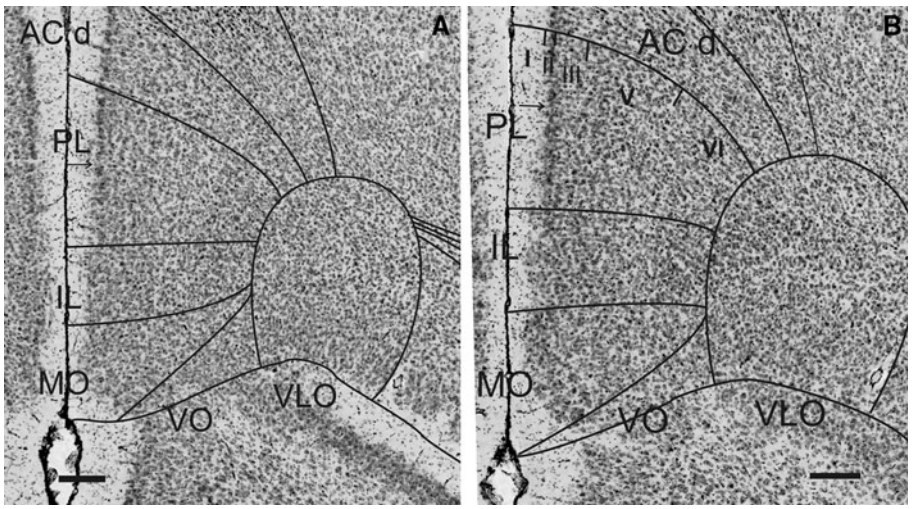

Fig. 6 **a** Ventral part of the medial PFC for details of the areas IL and MO; level: **e** in Fig. 2. In ACd, the layer II is characteristic, and the columns in layers V and VI are distinguishable albeit with some difficulty. Columns are absent in PL and layer VI of PL is denser. Layers II and III of the dorsal and ventral PL differ in density. Homogeneity of layers is characteristic in IL. In MO, the cells in layer II are equally dispersed. VLO is characterized by columns in layers II and III. **b** Medial PFC at a level between **e** and **i** in Fig. 2. In dorsal PL, layer II is narrower than in ventral PL. Layer VI in PL and IL have a more horizontal arrangement. In IL, homogeneity is mainly seen in layers II and III. In MO, the evenly dispersed cells in the well visible layer II is characteristic. VLO shows the characterizing columns and homogeneity of layers II and III. *Arrow* indicates the border between the dorsal and ventral PL. *Scale bars* 150 μm

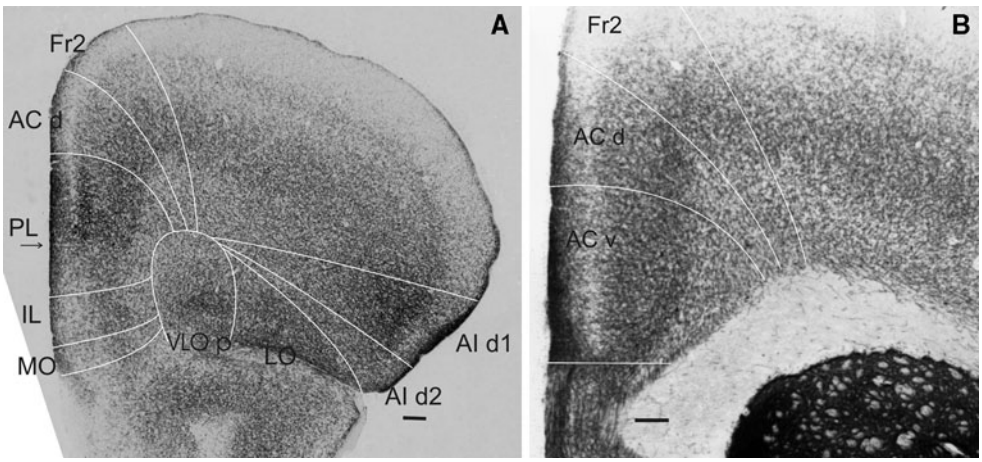

Fig. 7 Acetylcholinesterase staining. **a** Section through the frontal lobe. The strongest staining is in dorsal PL and in AId1. In ACd and Fr2, staining is mainly seen in layer V. Staining in the ventral PL, IL and MO is light and mainly in layer V. In VLOp, staining is mainly in the lateral part. In LO, staining is seen in layer V and in the superficial layers. Area AId2 shows less staining than its neighboring areas. *Arrow* indicates the border between the dorsal and ventral PL. **b** Medial PFC at the start of ACv. In ACd, staining is less than ACv and mainly deep in layer V; in Fr2, staining is less than in ACd. *Scale bars* 150 μm

Border between ventrolateral and ventral orbital areas

The characteristic of VLO is the columnar arrangement of the cells in layers II and III, whereas in VO layer II cells show a more disorderly appearance (Figs. 3, 4a, 8). VO is also the cortical area that provides the first contact between the frontal lobe and the retrobulbar region (Fig. 4a).

Border between ventral and medial orbital areas

In VO, layer II has a disorderly appearance with a vague border with layer III, while in MO the cells in layer II are evenly dispersed and layer II has a clearer boundary with layer III. The cortical layers are less distinct in VO than in MO, but this difference is small (Figs. 3, 4a, 8).

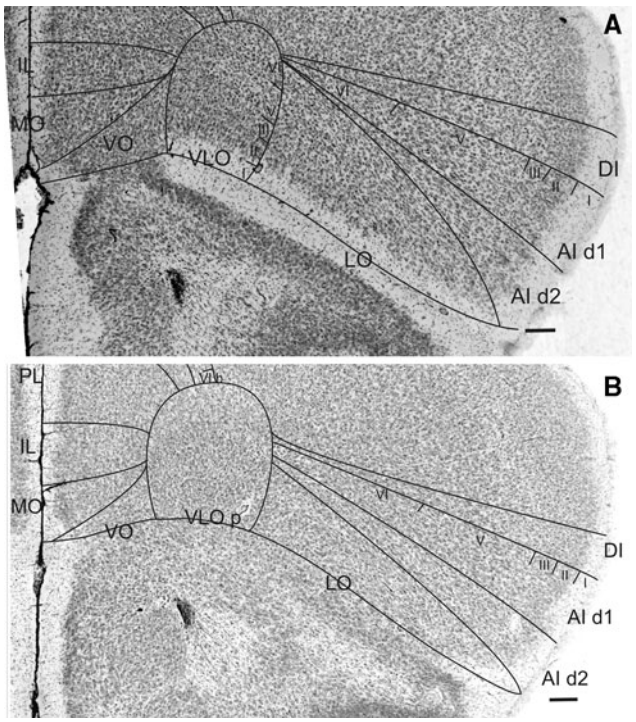

Fig. 8 **a** Orbital and lateral areas of the PFC at the anterior fusion of the frontal lobe with the retrobulbar region. Typical features are the columns and the homogeneity in the layers II and III of VLO, the clusters of cells in layer II of LO, the loose layer II of AId 2 with cells spreading into layer I and densely packed columns, the wide and rather homogeneous layer II of AId 1 and the less densely packed columns in the lower layers. **b** The same areas at a more posterior level: **f** in Fig. 2. Typical features are the homogeneity of IL, the sharply outlined layer II with evenly dispersed cells in MO and the homogeneity of VLOp. *Scale bars* 150 μm

Table 1 Comparison borders visible in different stainings

Borders	Nissl	AChE	SMI-32	SMI-311	Myelin	PV	Cb	DA
Fr1/Fr2	++							±
Fr2/ACd	++	±				+	+	+
ACd/PL	++	++			+	+	+	+
ACd/ACv	++	+			+	+	+	+
PL/IL	++	±					±	
PL/MO	++			++	++			
IL/MO	++						+	
DI/AId1	++	++			±	±		
AId1/AId2	++	++		±	±	+	±	++
AId1/AIp	++							
DI/AIp	++	++						
AId2/LO	++	++	++	++	++	++	+	++
LO/VLO	++	++	++	++	++	++	+	
VLO/VO	++			+	+	+	±	
VO/MO	++			+	±			
PFC/RS	++							

++ Clearly definable, + definable, ± difficult to define, *no symbol* not definable

Chemoarchitectonic features

We examined (immuno)cytochemical stainings to compare the borders visible in these stainings with those in Nissl-stained sections to determine to what extent cytochemical borders coincide with cytoarchitectonically defined PFC subareas. For comparison, we extrapolated the borders into these cytochemical stainings from Nissl-stained sections in the same mouse brain.

Acetylcholinesterase staining

In AChE-stained sections, the dorsal parts of PL and AId1 (Fig. 7a) are the most strongly stained areas in the precallosal PFC. In this staining, LO is more heavily stained than AId2, and the pattern of staining in LO differs from that in VLO (Fig. 7 a). In the supracallosal part of the PFC, the staining is strongest in ACv. It is less in ACd, and least in Fr2 (Fig. 7b). Table 1 summarizes the visibility of borders in the AChE staining: between the PFC areas only the borders ACd/PL, AId1/AId2 and AId2/LO are well detected with this staining.

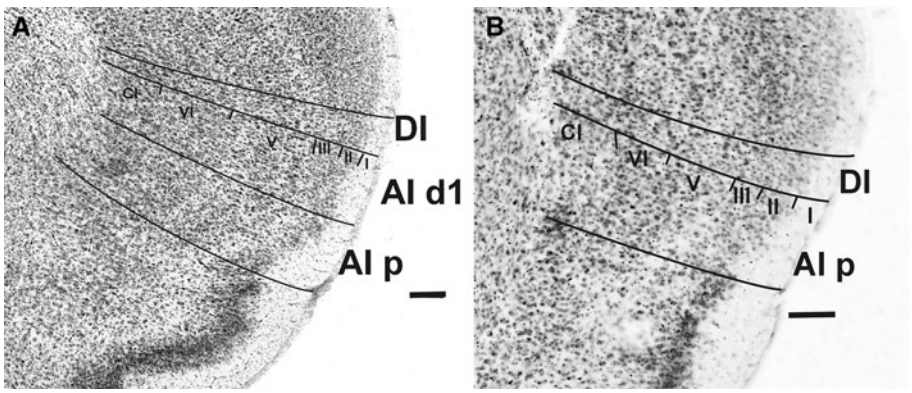

Fig. 9 **a** Lateral PFC at the transition to AIp. Typical are the clearly distinguishable (sub)layers of AIp and the columns in AId1. **b** *AIp* posterior to the PFC, *CL* claustrum. In DI, layers II, III and IV are homogeneous. *Scale bars* 150 μm

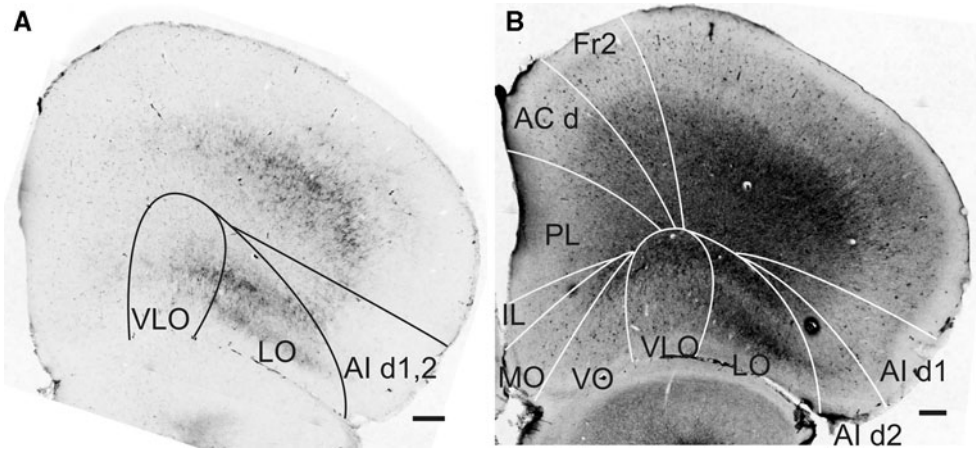

Fig. 10 **a** Section through the frontal lobe, stained by SMI-32. Layers III and V are well stained in LO. In VLO, staining is seen mainly in the lateral part; in AId, staining is limited to the deepest part of layer V; and in the medial PFC subareas, very sparse staining is present. **b** Section at the corresponding level, stained by SMI-311. Staining is strongest in LO, and in VLO staining is more in its lateral part. In Fr2, many large neurons are stained in layer V. PL shows less staining than ACd and Fr2. AId1 and AId2 show only few stained cells. *Scale bars* 150 μm

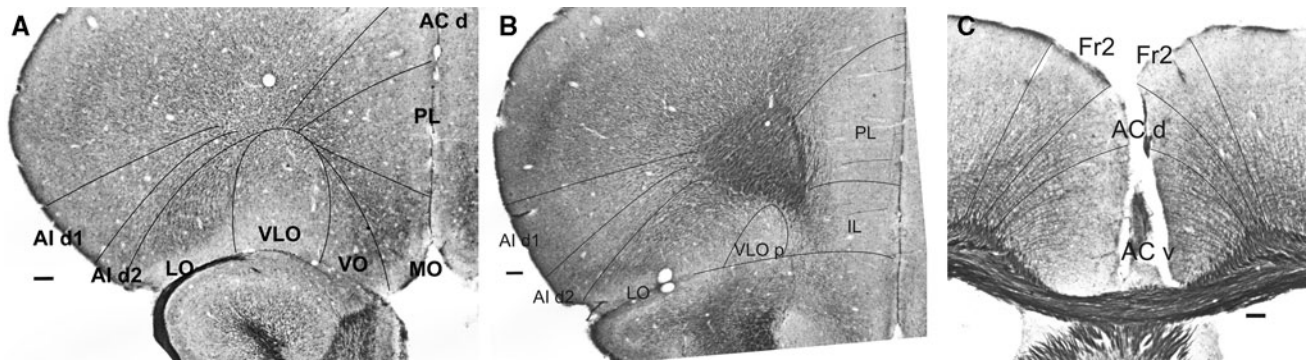

Fig. 11 Myelin-stained sections. **a** Section through the frontal lobe. Nerve fibers are most strongly stained in LO. Sparsest staining is present in VLO. **b** At the level of the forceps minor of the corpus callosum. The nerve fibers are most strongly stained in LO. **c** Supracallosal PFC. Longest and most densely packed fibers are seen in Fr2 and ACd; in ACv, fibers are shorter and less densely packed. *Scale bars* 150 μm

SMI-32 and SMI-311

The lack of SMI-32 staining in most areas of the mouse PFC is striking (Fig. 10a). Only in LO, some layers display clear immunopositive reaction. In VLO, less staining is present.

In the corresponding SMI-311 section (Fig. 10b), the strongest staining is also seen in LO. In VLO, the deeper layers are well stained, but staining of layer III is much less than in LO. Table 1 summarizes that in SMI-32 sections only the borders of LO with AId2 and with VLO are well defined and in SMI-311, in addition, the border PL/MO in the anterior part of the frontal lobe.

Myelin staining

In the myelin-stained sections, VLO and VLOp are conspicuous by the paucity of staining. (Fig. 11a, b), while LO is more heavily myelinated. The myelin staining in VO and MO is also much stronger than in VLO (Fig. 11a, b). Figure 11b shows that PL is not differentiated from IL; both are lightly myelinated. The myelinization in ACd appears stronger than in PL (e.g., Fig. 11b).

In the supracallosal region of the PFC, the length and density of fibers are larger in ACd and Fr2 than in ACv (Fig. 11c).

Table 1 summarizes that in myelin-stained sections only the borders of LO with VLO and with AId2 are clearly definable.

Parvalbumin

In the precallosal region of the PFC, the strongest and most general PV staining is in LO (Fig. 12a). The staining in VLOp is stronger and more general than in VLO (Fig. 12a, b). The staining in AId2 tends to be stronger than in AId1

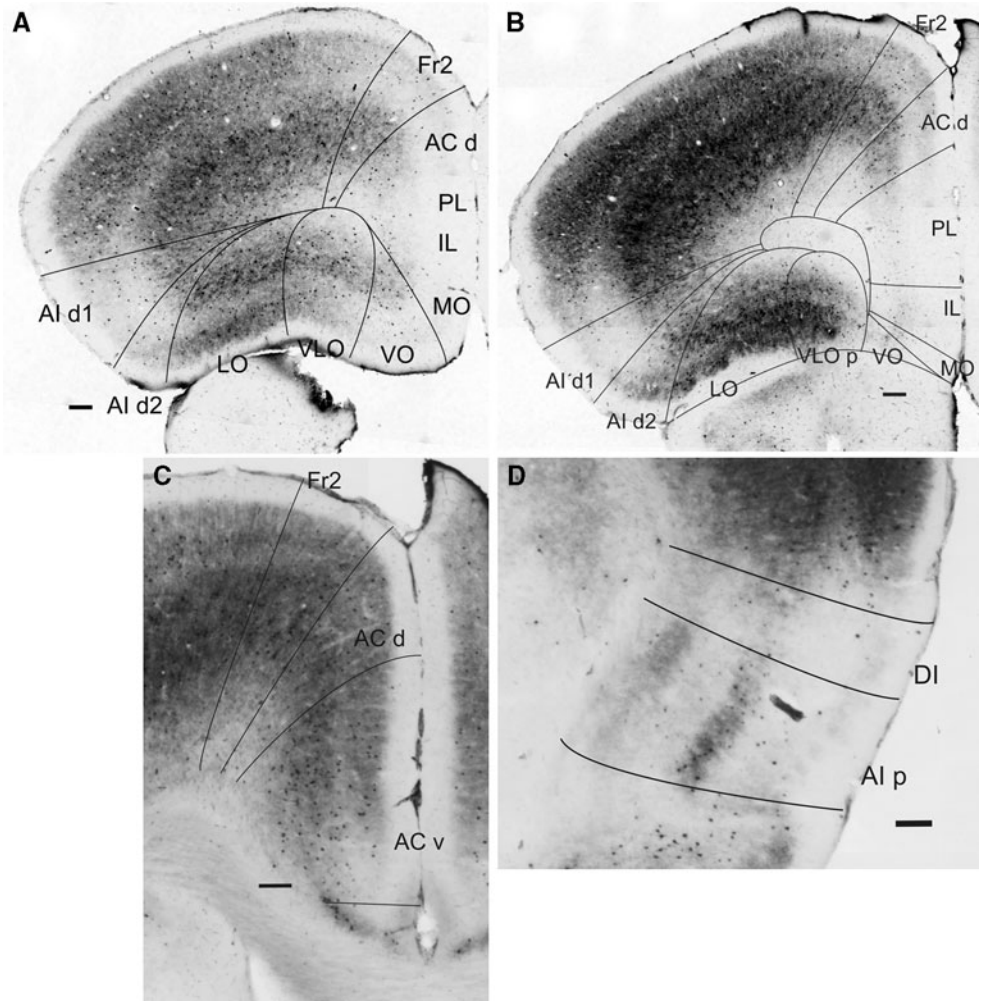

Fig. 12 Parvalbumin-stained sections. **a** Level of the frontal lobe. Strongest staining in LO and lateral part of VLO. In AId1 and AId2, sparse cells are seen in nearly all the layers. This is also seen in VO. **b** Level after fusion of the frontal lobe with the retrobulbar region. Strongest staining in LO and VLOp. Staining of cells in deep layers more in AId2 than in AId1. **c** Supracallosal PFC. Parvalbumin-positive cells in ACv are much more packed than in ACd or Fr2. **d** Level of AIp. Most cells are seen in layer V of AIp. *Scale bars* 150 μm

(Fig. 12b). In general, PV staining in the medial PFC is poor, but in the more posterior sections Fr2 and ACd show stronger staining (Fig. 12a, b). No border is visible between PL, IL and MO in PV-stained sections (Fig. 12a, b).

In the supracallosal part of the PFC, the PV staining is heaviest in Fr2, less in ACd and least in ACv, especially in the ventral part of ACv (Fig. 12c). The highest density of PV-positive cells is, however, visible in layer V of ACv, especially in the dorsal part (Fig. 12c).

In AIp, the pattern of PV-stained layers shows a higher PV-positive lamination than in AId1, which resembles Nissl-stained sections (Fig. 12d).

Table 1 summarizes that only the borders of LO with AId2 and with VLO are well detectable in PV stainings.

Calbindin

Differences of pattern and intensity of CB staining corroborate the PFC areas extrapolated from Nissl sections, but they are much less distinctive than in Nissl staining (Fig. 13a–c). Table 1 summarizes that between PFC areas in CB-stained sections, no border is consistently clearly definable.

Dopamine

Dopamine staining is present in most areas of PFC except for VLO, LO and the part of VO anterior to the fusion of the frontal lobe with the retrobulbar region (Figs. 14a, 15). At the fusion of the retrobulbar region with VO,

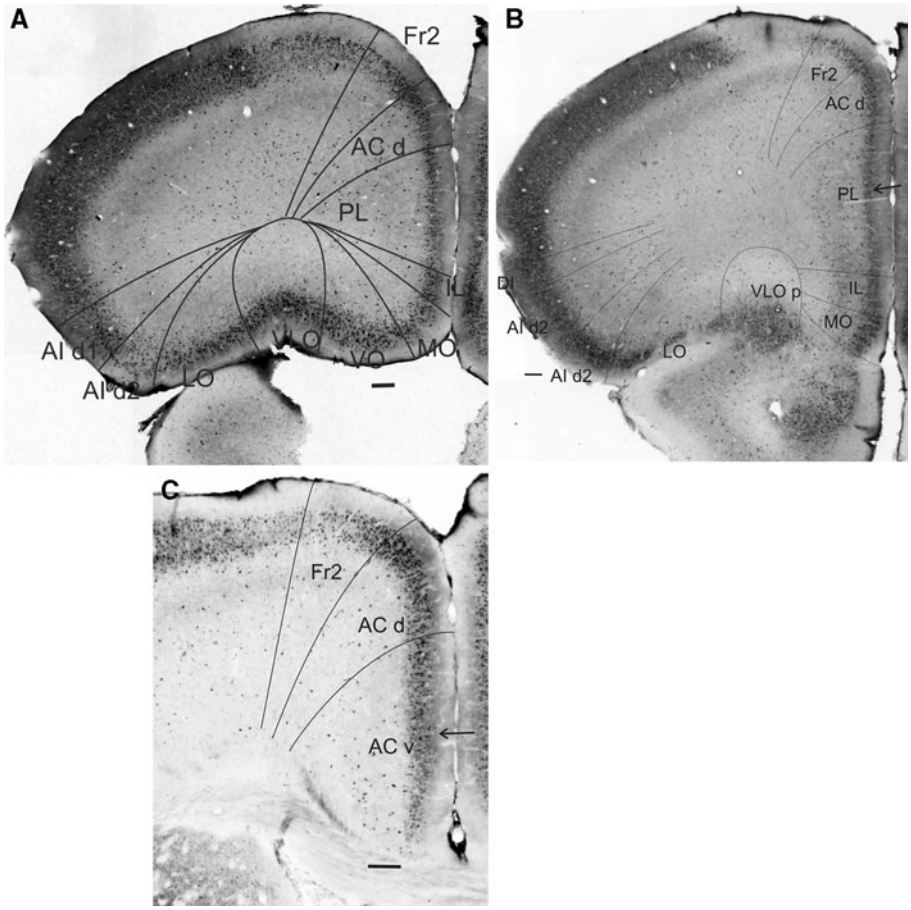

Fig. 13 Calbindin-stained sections. Boundaries have been extrapolated from Nissl-stained sections. Except for columns and densely packed cells in VLO and clustering of cells in LO and MO, typical features for identifying areas are not abundant. **a** Level of frontal pole. Small cells in AId2, clusters in layer II in LO, and in VLO densely packed cells and columns. **b** Level after fusion of the frontal lobe with the retrobulbar region. Densely packed cells in AId2, clusters of cells in LO and homogeneity of cells in VLOp. *Arrow* indicates border between the dorsal and ventral PL. **c** Supracallosal PFC. Concentration of cells of layer II at the boundary with layer I characterizes ACd. No strong staining in Fr2 and ACv. *Arrow* indicates the border between the dorsal and ventral ACv, extrapolated from Nissl staining in the adjacent section. *Scale bars* 150 μm

dopaminergic fibers run through VO (Fig. 14b), as in the rat (Van de Werd and Uylings 2008). In the supracallosal region, the staining of ACv is stronger than in ACd and Fr2 (Fig. 14c). In the anterior part of PL, the dopaminergic fibers run mainly in layers II and V (Fig. 14a), while in the PL part caudal to the fusion of the frontal lobe with the retrobulbar region, the dopaminergic fibers are mainly in layer VI (Fig. 14b). This laminar pattern differs from the one in the AId2. In fact, in AId2 the dopaminergic fibers are in all layers with a slight preference for the deeper and the upper part of the cortex (Fig. 15). As in the rat, less dopaminergic fibers are present in the mouse claustrum in comparison to the AIp layers (Fig. 15c).

Table 1 summarizes, that in dopamine-stained sections, the borders of AId2 with AId1 and with LO are clearly detectable.

Discussion

"Results" and Table 1 demonstrate that to define mouse prefrontal areas, cytoarchitectonic staining is preferred to cytochemical stainings as in rat (Van De Werd and Uylings 2008) and human (Őngür et al. 2003) studies. Cytochemical staining did show two or more borders of mouse PFC areas clearly, but cytochemical staining did not show all the borders definable in Nissl sections. Taking all the cytochemical stainings together, 7 of the 14 borders are clearly detectable (Table 1). The PFC areas clearly definable in cytochemical stainings are LO, AId1 and AId2, and largely VLO and PL. LO, as defined in Nissl staining, is visible in SMI 32 and SMI 311 because of its double-layered staining, as in AChE and in PV staining. LO is also more strongly myelinated. AId1, as defined in Nissl staining, is well definable in AChE staining, and also as a very sparsely stained AId1 in the PV staining. AId2, as defined in Nissl staining, is recognizable in dopamine staining by the abundant DAergic fibers, which are much less dense in the neighboring areas. In AChE staining, however, AId2 is much less stained than the neighboring AId1 and LO. VLO, as defined in Nissl-stained sections, is visible in CB because of its columnar pattern, and in dopamine staining due to a lack of dopaminergic fibers. PL, as defined in Nissl staining, is detectable in dopamine staining by its strong staining of layers II and V. Dorsal PL is corroborated by the three strongly stained layers seen in dorsal PL in AChE staining.

Our nomenclature of the subareas of the PFC in the mouse corresponds, in general, to the one Ray and Price

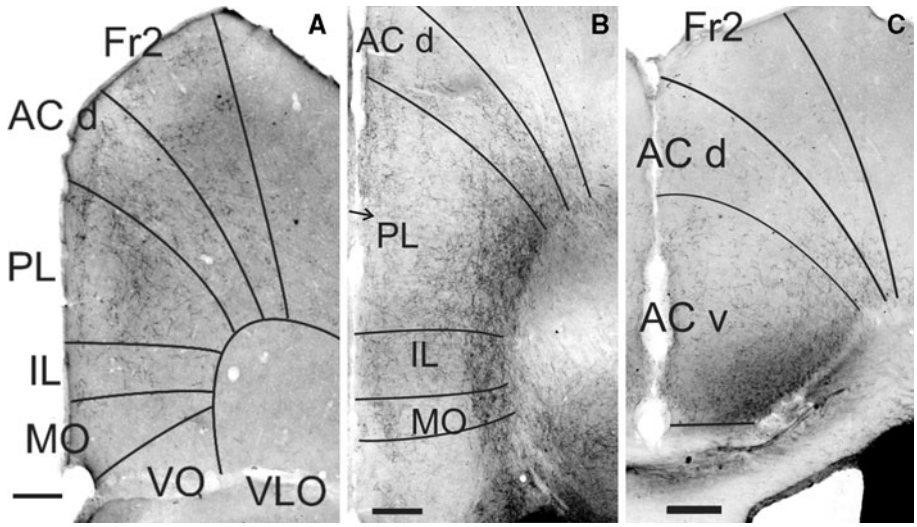

Fig. 14 Dopamine-stained sections. **a** Frontal lobe. Dopamine-stained fibers present in all areas of the medial PFC, especially in PL. **b** Medial PFC at the pregenual level. Dopaminergic fibers in all areas of the medial PFC, especially in layer VI in PL. *Arrow* indicates the border between the dorsal and ventral PL, extrapolated from Nissl staining in the adjacent section. Fiber density in layer V in the ventral PL was higher than that in the dorsal PL. **c** Supracallosal PFC. Dopaminergic fibers were mostly in ACv and less in ACd and Fr2. *Scale bars* 150 μm

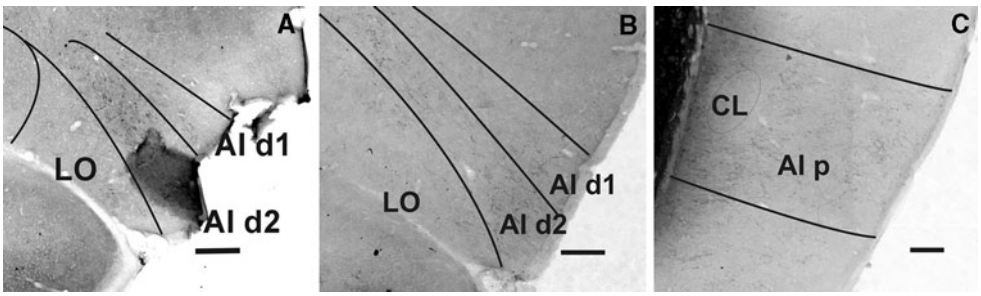

Fig. 15 Dopamine staining. **a** The abundance of dopaminergic fibers in AId2. **b** Dopaminergic fibers are abundant in AId2 and less in AId1 and LO. **c** AIp shows dopaminergic fibers in all layers, but no dopamine is seen in the claustrum. *Scale bars* 150 μm

(1992) used for the rat PFC, but differs in the following aspects. We prefer using the neutral name of Fr2 as introduced by Zilles (1985) instead of the medial precentral area (PrCm), since the mouse and rat do not have a central sulcus (Uylings and Van Eden 1990). The terms lateral and medial frontal polar subareas (Ray and Price 1992), i.e., FP_l and FP_m, respectively, are not adopted by us, since we can extrapolate the prefrontal cortical areas into this frontopolar region. As we did in the rat PFC (Van de Werd and Uylings 2008), we define two subareas in the mouse AId, i.e., AId1 and AId2. In contrast to the rat PFC, we could not distinguish a dorsolateral orbital area (DLO) in the mouse among AId in a reproducible way, nor could we distinguish a ventral agranular insular subarea (AIv) among LO. In mouse, we prefer the term AId and LO on the basis of its architectonic structure, which is more like the rat AId and LO than the rat DLO and AIv, respectively (Van de Werd and Uylings 2008). In the mouse, LO maintains its features from the rostral to the caudal end, while in the rat, LO is replaced caudally by an area AIv. This area is characterized by a layer III, which is very cell-sparse compared to layer III in LO. In general, such a change from LO into AIv is not detected in the mouse brain. Therefore, we prefer defining the whole area as LO and have not specified an AIv area in the mouse.

An important macroscopic aspect of the mouse frontal lobe is the very short frontal pole that is detached from the retrobulbar region. This is different from the rat frontal pole, which is (relatively) longer. In fact, the anterior–posterior distance of the free part of the mouse frontal lobe is hardly as large as the thickness of the six layers of the cortex. Therefore, the characteristics of the superficial layers have been used by us to distinguish the prefrontal areas in the frontal pole in the coronal sections. Yet on the basis of our experience with rat brains cut in coronal, sagittal and horizontal planes, coronal sections are preferred by us for PFC area definition.

The cytoarchitectonic characteristics described in this study are also visible in the "Atlas of the Mouse Brain" by Franklin and Paxinos. This does not mean that all PFC areas defined in this study are similar to the areas specified in this atlas. We agree repeatedly for AId1, AId2, LO, VLO, IL, PL, ACd and ACv, but differ for MO, Fr2 and AIp. We also note that AId2 is called AIv in Franklin and Paxinos (2008). We prefer the term AId2, since AIv is located inside the rhinal sulcus in rat PFC studies (e.g., Uylings and Van Eden 1990; Ray and Price 1992; Reep et al. 1996; Uylings et al. 2003; Van De Werd and Uylings 2008). In a following study (Van de Werd and Uylings, in preparation), we will review in detail with maps the

similarities and differences of the prefrontal areas defined in this study with the mouse stereotaxic atlases (Hof et al. 2000; and Franklin and Paxinos 2008), the mouse cytoarchitectonic atlas by Rose (1929) and the mouse cytoarchitectonic studies by Caviness (1975) and Wree et al. (1983).

In comparing mouse studies, it will be important to consider whether size and defining features of the prefrontal areas differ between different genetic/inbred mouse strains (Leingärtner et al. 2007). Strain differences in the visual cortex and the 'barrel' cortex, but not between the entire size of the somatosensory cortex and the auditory cortex, have been reported between C57BL/6J and DBA/2J (Airey et al. 2005). On the basis of the figures of Hof et al. (2000), we can expect differences in the ACv areas of the 129/Sv strain.

The prefrontal cortical areas can only be defined as such on the basis of reciprocal connectivity patterns with the dorsomedial nucleus of the thalamus, the intralaminar thalamic nuclei, the neocortical areas, the basal ganglia, the hypothalamus and the brain stem (Uylings et al. 2003). To date, little is known about such connectivity patterns in the mouse brain. Only one mouse study was published 29 years ago on the connections of the medial and lateral PFC with the mediodorsal nucleus of the thalamus (Guldin et al. 1981). This study demonstrates that the medial and lateral 'PFC' areas receive mediodorsal connections. For area AC_v, however, such connections were not detected in this study, but more refined tracing techniques have been developed afterward. In the rat, the reciprocal projection pattern of AC_v with the mediodorsal thalamic nucleus was also revealed in a later, more extensive study by Groenewegen (1988). By extrapolating the rat tracing studies it is quite likely that the cytoarchitectonic cortical areas described here are indeed prefrontal areas, with the possible exception of VLO (Reep et al. 1996; Uylings et al. 2003). It is still debatable whether the VLO area in the rat can be considered to be part of PFC. On the basis of current knowledge of connectivity patterns (Cechetto and Saper 1987; Ray and Price 1992; Uylings et al. 2003), in the rat brain the DI is not considered to be part of the PFC. Detailed tracing studies are necessary to further establish whether or not the cytoarchitectonically defined frontal mouse areas are all prefrontal areas indeed. Our study provides an appropriate description of the characteristics of the cytoarchitectonic delineation of these cortical areas that can be applied to future detailed tracing studies, which can be expected from a large US program on comparative mouse neuroanatomy (Bohland et al. 2009).

Future tracing studies will demonstrate whether DLO and AId, and LO and AIv, respectively, are 'intermingled' in the mouse, or whether a DLO and an AIv can be distinguished from AId and LO, respectively. In the rat, AId projects onto the core of the accumbens nucleus, whereas DLO projects more to the dorsolateral striatum (Fig. 2 in Groenewegen and Uylings 2010) and LO projects to the lateral striatum, whereas AIv projects to the lateral accumbens shell and ventral to this area (Fig. 2 in Groenewegen and Uylings 2010).

In conclusion, the cytoarchitectonic definitions of mouse prefrontal cortical areas described in this study will be of use in stereological studies (e.g., Rajkowska et al. 2004) for which borders of individual areas have to be determined to estimate the total number of neurons and/or glial cells. Moreover, these cytoarchitectonic criteria will be very useful for a more precise localization of recording electrodes (e.g., Herry and Garcia 2002), microdialysis probes (e.g., Van Dort et al. 2009), receptor binding sites and mRNAs expression (e.g., Amargós-Bosch et al. 2004; Lidow et al. 2003), as well as for anatomical guidance of neuroimaging studies (e.g., Barrett et al. 2003) and tracing neural connections to and from mouse frontal cortical areas.

Acknowledgments We thank Mrs. G. Clarke for the preparation of histological Nissl-stained sections, Mr. H. Stoffels for his drawings in Fig. 1 and Dr. L.J.A. Huisman for correcting the English. This study was supported by Grants RO1 MH61578 (G.R.; H.B.M.U.), MH60451 (GR) and RR17701 (GR).

References

Airey DC, Robbins AI, Enzinger KM, Wu F, Collins CE (2005) Variation in the cortical area map of C57BL/6J and DBA/2J inbred mice predicts strain identity. BMC Neurosci 6:18

Amargós-Bosch M, Bortolozzi A, Puig MV, Serrats J, Adell A, Celada P, Toth M, Mengod G, Artigas F (2004) Co-expression and in vivo interaction of serotonin1A and serotonin2A receptors in pyramidal neurons of prefrontal cortex. Cereb Cortex 14:281–299

Barrett D, Shumake J, Jones D, Gonzalez-Lima F (2003) Metabolic mapping of mouse brain activity after extinction of a conditioned emotional response. J Neurosci 23:5740–5749

Bohland JW, Wu C, Barbas H, Bokil H, Bota M et al (2009) A proposal for a coordinated effort for the determination of brainwide neuroanatomical connectivity in model organisms at a mesoscopic scale. PLoS Comput Biol 5(3):e1000334. doi: 10.1371/journal.pcbi.1000334

Cavada C, Comañy T, Hernández-González A, Reinoso-Suárez F (1995) Acetylcholinesterase histochemistry in the macaque thalamus reveals territories selectively connected to frontal, parietal and temporal association cortices. J Chem Neuroanat 8:245–257

Caviness VS Jr (1975) Architectonic map of neocortex of the normal mouse. J Comp Neurol 164:247–263

Cechetto DF, Saper CB (1987) Evidence for a viscerotopic sensory representation in the cortex and the thalamus in the rat. J Comp Neurol 262:27–45

De Brabander JM, Van Eden CG, De Bruin JPC, Feenstra MGP (1992) Activation of mesocortical dopaminergic system in the rat in response to neonatal medial prefrontal cortex lesions. Concurrence with functional sparing. Brain Res 581:1–9

Franklin KJ, Paxinos G (2008) The mouse brain in stereotaxic coordinates, 3rd edn. Academic Press, San Diego

Gallyas F (1979) Silver staining of myelin by means of physical development. Neurol Res 1:203–209

Geffard M, Buijs RM, Seguela P, Pool CW, Le Moal M (1984) First demonstration highly specific and sensitive antibodies against dopamine. Brain Res 294:161–165

Groenewegen HJ (1988) Organization of the afferent connections of the mediodorsal thalamic nucleus in the rat, related to mediodorsal-prefrontal topography. Neuroscience 24:379–431

Groenewegen HJ, Uylings HBM (2010) Organization of prefrontal-striatal connections. In: Steiner H, Tseng KY (eds) Handbook of basal ganglia structure and function. Academic Press, San Diego

Groenewegen HJ, Witter MP (2004) Thalamus. In: Paxinos G (ed) The rat nervous system, 3rd edn. Academic Press, San Diego, pp 407–453

Guldin WO, Pritzel M, Markowitsch HJ (1981) Prefrontal cortex of the mouse defined as cortical projection area of the thalamic mediodorsal nucleus. Brain Behav Evol 19:93–107

Herry C, Garcia R (2002) Prefrontal cortex long-term potentiation, but not long-term depression, is associated with the maintenance of extinction of learned fear in mice. J Neurosci 22:577–583

Hof PR, Young WG, Bloom FE, Belichenko PV, Celio MR (2000) Comparative cytoarchitectonic atlas of the C57BL/6 and 129/Sv Mouse Brains. Elsevier, Amsterdam

Kalsbeek A, De Bruin JPC, Feenstra MGP, Uylings HBM (1990) Age-dependent effects of lesioning the mesocortical dopamine system upon prefrontal cortex morphometry and PFC-related behaviors. Prog Brain Res 85:257–282

Krettek JE, Price JL (1977) The cortical projections of the mediodorsal nucleus and adjacent thalamic nuclei in the rat. J Comp Neurol 171:157–191

Leingärtner A, Thuret S, Kroll TT, Chou S-J, Leasure JL, Gage FH, O'Leary DDM (2007) Cortical area size dictates performance at modality-specific behaviors. Proc Natl Acad Sci USA 104:4153–4158

Lidow MS, Koh PO, Arnsten AFT (2003) D1 dopamine receptors in the mouse prefrontal cortex: immunocytochemical and cognitive neuropharmacological analyses. Synapse 47:101–108

Őngür RD, Ferry AT, Price JL (2003) Architectonic subdivision of the human orbital and medial prefrontal cortex. J Comp Neurol 460:425–449

Rajkowska G, Dubey P, Clarke G, Ni Thuairisg S, Mahajan G, Licht C, van de Werd HJJM, Miguel-Hidalgo JJ, Yuan P, Manji HK, Uylings HBM (2004) Glial number is increased in hippocampus, but not in prefrontal cortex in lithium-treated mice: a stereological study. Int J Neuropsychopharmacol 7:S360

Ray JP, Price JL (1992) The organization of the thalamocortical connections of the mediodorsal thalamic nucleus in the rat, related to the ventral forebrain-prefrontal cortex topography. J Comp Neurol 323:167–197

Reep RL, Corwin JV, King VR (1996) Neural connections of orbital cortex in rats: topography of cortical and thalamic afferents. Exp Brain Res 111:215–232

Rose M (1929) Cytoarchitektonischer Atlas der Großhirnrinde der Maus. J Psychol Neurol 40:1–51

Slotnick BM, Leonard CM (1975) A stereotactixic atlas of the albino mouse forebrain. US Dept. Health Education & Welfare, Rockville

Uylings HBM, Van Eden CG (1990) Qualitative and quantitative comparison of the prefrontal cortex in rat and in primates, including humans. Prog Brain Res 85:31–62

Uylings HBM, Groenewegen HJ, Kolb B (2003) Do rats have a prefrontal cortex? Behav Brain Res 146:3–17

Van De Werd HJJM, Uylings HBM (2008) The rat orbital and agranular insular prefrontal cortical areas: a cytoarchitectonic and chemarchitectonic study. Brain Struct Funct 212:387–401

Van Dort CJ, Baghdoyan HA, Lydic R (2009) Adenosine A(1) and A(2A) receptors in mouse prefrontal cortex modulate acetylcholine release and behavioral arousal. J Neurosci 29:871–881

Van Eden CG, Uylings HBM (1985) Cytoarchitectonic development of the prefrontal cortex in the rat. J Comp Neurol 241:253–267

Wree A, Zilles K, Schleicher A (1983) A quantitative approach to cytoarchitectonics. VIII. The areal pattern of the cortex of the albino mouse. Anat Embryol 166:333–353

Zilles K (1985) The cortex of the rat. A stereotaxic atlas. Springer, Berlin